10-29-2022

Terminal field volume of the glossopharyngeal nerve in adult rats reverts to prepruning size following microglia depletion with PLX5622

Andrew J. Riquier
University of Nebraska at Omaha, ariquier@unomaha.edu

Suzanne I. Sollars
University of Nebraska at Omaha, ssollars@unomaha.edu

Recommended Citation

WILEY

Terminal field volume of the glossopharyngeal nerve in adult rats reverts to prepruning size following microglia depletion with PLX5622

Andrew J. Riquier [ORCID] | Suzanne I. Sollars

Department of Psychology, University of Nebraska at Omaha, Omaha, Nebraska, USA

Correspondence
Suzanne I. Sollars, Department of Psychology, University of Nebraska at Omaha, 6001 Dodge Street, 419 Allwine Hall, Omaha, NE 68182, USA.
Email: ssollars@unomaha.edu

Abstract

Programmed reduction of synapses is a hallmark of the developing brain, with sensory systems emerging as useful models with which to study this pruning. The central projections (terminal field) of the gustatory glossopharyngeal nerve (GL) of the rat are a prime example of developmental pruning, undergoing an approximate 66% reduction in volume from postnatal day 15 (P15) to P25. Later in adulthood, developmental GL pruning can be experimentally reversed, expanding to preweaning volumes, suggesting mature volumes may be actively maintained throughout the life span. Microglia are central nervous system glia cells that perform pruning and maintenance functions in other sensory systems, including other gustatory nerves. To determine their role in GL pruning, we depleted microglia from Sprague–Dawley rat brains from P1 to P40 using daily intraperitoneal injections of the colony-stimulating factor 1 receptor inhibitor PLX5622. This prevented GL developmental pruning, resulting in preweaning terminal field volumes and innervation patterns persisting through P40, 2 weeks after pruning is normally completed. These findings show microglia are necessary for developmental GL pruning. Ceasing PLX5622 treatments at P40 allowed microglia repopulation, and within 4 weeks the GL terminal field had reduced to control volumes, indicating that pruning can occur outside of the typical developmental period. Conversely, when microglia were depleted in adult rats, GL terminal fields expanded, reverting to sizes comparable to the neonatal rat. These data indicate that microglia are required for GL pruning and may continue to maintain the GL terminal field at a reduced size into adulthood.

KEYWORDS
astrocytes, colony-stimulating factor 1 receptor, development, gustatory, pruning

1 | INTRODUCTION

A critical stage of postnatal neural development is the selective elimination of surplus synapses, referred to as synaptic pruning, which occurs in rodents during the first 3–5 postnatal weeks (Neniskyte & Gross, 2017; Sun et al., 2019). Age-dependent innervation and synapse reduction have been observed in multiple brain regions such as the cerebellum (Hashimoto & Kano, 2003, 2013), cortex (Hoshiko et al., 2012; Low et al., 2008; Mallya et al., 2019), and brainstem (Mangold & Hill, 2008; Sollars et al., 2006). Sensory systems have emerged as a common model with which to study pruning, with robust and predictable pruning observed in the visual (Bialas & Stevens, 2013; Huberman, 2007; Innocenti, 1981; Schafer et al., 2012; Stevens et al., 2007), auditory (Milinkeviciute et al., 2019), and gustatory systems (Mangold & Hill, 2008; Sollars et al., 2006; Sun et al., 2019). In the nucleus of the solitary tract (NTS), the central projections (terminal field) of the rat gustatory glossopharyngeal nerve (GL) reduce in volume by ∼66% between postnatal day 15 (P15) and P25 (Mangold & Hill, 2008). This reduced terminal field volume is stable for the remainder of life, yet expansion in adulthood to prepruning volumes can be induced by both systemic and taste receptor cell-specific removal of brain-derived neurotrophic factor (Sun et al., 2018). Together, these findings suggest the GL may not merely be pruned, but actively maintained at a reduced size, a maintenance that can be disrupted.

Glia cells of the central nervous system (CNS) are known to be active contributors to the developmental pruning process. Astrocytes prune retinogeniculate synapses both during early development and adulthood via the phagocytic MEGF10 and MERTK pathways based on neural stimulation (Chun et al., 2013). Besides direct synaptic engulfment, astrocytes also secrete TGF-β, which initiates a cascade that culminates in pruning by microglia, ubiquitous self-renewing immune cells of the CNS (Askew et al., 2017; Bialas & Stevens, 2013; Bruttger et al., 2015). Microglia prune synapses during early postnatal development in an activity- and complement-dependent manner (Paolicelli et al., 2011; Schafer et al., 2012; Stevens et al., 2007). Later in life, microglia are required for motor-learning-dependent synapse formation in early adulthood (Parkhurst et al., 2013), maintaining retinal photoreceptor synapses in the external plexiform layer (Wang et al., 2016), and continue to regularly contact and influence neurons in the adult brain (reviewed in Kierdorf & Prinz, 2017).

While microglia are required for developmental pruning of the gustatory branches of the facial nerve in mice (Sun et al., 2019), their role and that of astrocytes in rat GL pruning and maintenance have yet to be established. As both microglia and astrocyte quantities are elevated in regions undergoing synaptic pruning (Bialas & Stevens, 2013; reviewed in Schafer & Stevens, 2015; Sun et al., 2019), in the current study glia densities in the NTS were assessed during periods of GL development. To determine if microglia are required for GL terminal field pruning, microglia were depleted from the rat brain using the colony-stimulating factor 1 receptor (CSF1R) inhibitor PLX5622 (Plexxikon, Inc.) from P1 to P40 and the volume of the GL NTS terminal field was analyzed at key stages of development. In order to test the flexibility of the pruning period, treatments were ceased in a subgroup of rats treated with PLX5622 from P1 to P40, allowing the microglia to repopulate, and GL NTS terminal fields were assessed. Microglia were also depleted in a group of postpruning adult rats to see if microglia actively maintain the GL terminal field at a reduced volume.

2 | METHODS

2.1 | Subjects

Every condition included nearly equal quantities of both male and female Sprague–Dawley rats (*Rattus norvegicus*; total $N = 131$) randomly assigned from at least two litters, bred in the University of Nebraska at Omaha Vivarium (see Table 1 for specific conditions). Rats were socially housed in clear Plexiglass cages on a 12:12 light–dark cycle with free access to tap water and food pellets (Teklad). Day of birth was denoted as postnatal day 0 (P0), and rats were weaned at P25. To facilitate comparable nutrition across litters and development, all experimental litters contained between seven and 12 pups through weaning. To both monitor health and collect data on weight changes during development, all rats were weighed daily for the duration of the experiment. All animal procedures were approved by the University of Nebraska at Omaha Institutional Animal Care Committee's and conformed to the guidelines set forth by the National Institutes of Health and the United States National Research Council.

2.2 | Long-term intraperitoneal PLX5622 treatment in rat pups

The colony-stimulating factor 1 receptor (CSF1R) is unique to myeloid lineage cells (reviewed in Hume et al., 2020) and is required for both microglia survival (Elmore et al., 2015) and proliferation (Askew et al., 2017). Chow-based PLX5622 treatment rapidly depletes microglia in P18 mouse pups (Sun et al., 2019). However, our study necessitated microglia depletion by P14, as pruning was expected to occur at P15 (Mangold & Hill, 2008). Microglia depletion in embryonic and preweaning mice can be achieved by feeding PLX5622 to the dam, but this results in increased mortality

TABLE 1 Sample sizes for experimental conditions

Pruning					
Age (days)	14	25	40	68 developmentally treated	68 adult treated
PLX5622	6	5	5	4	5
Vehicle	4	4	5	3	
72 of transport			2		
Glia	**Across**	**Development**			
Age (days)	11	14	17	25	31–40
Microglia	7	N/A	4	4	5
Astrocytes	N/A	9	N/A	10	9
Chronic	**Microglia**	**Depletion**			
Age (days)	4	14	24	40	43 repopulated
PLX5622	4	6	5	5	3
Vehicle	2	5	5	5	N/A

and health complications for the pups (Rosin et al., 2018). Further, chow-based PLX5622 administration is less effective in rats than mice, and indirect administration makes exact dosing a challenge.

Starting at P1, rat pups received once daily intraperitoneal (i.p.) injections of 0.65% PLX5622 suspended in 5% dimethyl sulfoxide and 20% Kolliphor RH40 in 0.01 M phosphate-buffered saline (PBS) to a dose of 50 mg/kg. Microglia densities in the NTS were assessed by dividing raw microglia numbers by the volume of the NTS for a given animal. Pilot testing demonstrated that while this dose reduced microglia by >97% within 3 days and >99% by 7 days, by 10 days of age depletion had reduced to 75%. Therefore, starting at P12 rat pups received 50 mg/kg injections twice daily 10–12 h apart at Zeitgeber Time 2 and 12–14, respectively. During pilot testing, the efficacy of PLX5622 in depleting microglia appeared to diminish each week of continuous treatment, which could be compensated for by increasing the concentration of PLX5622 by 20% every 5 days for the remainder of the treatment period. Dimethyl sulfoxide (DMSO) and Kolliphor RH40 quantities were increased as necessary to suspend the PLX5622 in 0.01 M PBS. Vehicle animals received control injections containing identical concentrations of DMSO and Kolliphor RH40 in 0.01 M PBS. For the GL labeling studies, rats were treated P1–40, with a subgroup of animals then ceasing treatments for 4 weeks. Additionally, a final condition of rats was treated with PLX5622 only from P40 to P68.

2.3 | GL label

The GL of rats treated with PLX5622 or vehicle was labeled at P14, P25, P40 (n = 4-6/condition), or P68 (n = 3–5/condition). Animals were anesthetized with i.p. injections of Brevital Sodium (60 mg/kg) and a small incision was made

on the ventral portion of the neck. The GL was located medial and ventral to the tympanic bulla and cut, and DMSO followed by biotinylated dextran amine (BDA) (Invitrogen, BDA-3000) was applied to the nerve for 15 min. The incision was sutured, and animals were monitored until sternal recumbency was observed and then returned to their home cages. Animals were given 5 mg/kg carprofen i.p. after the surgery and 24 h later.

2.4 | Perfusion, tissue extraction, and sectioning

Forty-eight hours after surgery, animals were injected with a mixture of ketamine/xylazine and transcardially perfused with a modified Krebs solution (pH 7.3–7.35) followed by 8% paraformaldehyde. Brains were extracted and postfixed in 8% paraformaldehyde overnight. Using a vibrating microtome, brains were sectioned horizontally at 50 μm (nerve label) or 40 μm (immunohistochemistry; separate sections for ionized calcium-binding adapter molecule 1 [Iba1] or glial fibrillary acidic protein [GFAP]). All processing was performed on free-floating sections.

2.5 | Nerve label processing

All rinses and incubations were performed with 0.1 M PBS (pH 7.5). Following five 5-min rinses, sections were placed in a 1% triton solution (4 × 15 min), then incubated with a 2% avidin–biotin complex solution containing 0.1% Triton X-100 for 2 h (PK-6100; Vector Laboratories, Burlingame, CA). Sections were then rinsed (3 × 15 min) and placed in a 0.05% diaminobenzidine/0.125% nickel ammonium sulfate solution containing 0.01% H_2O_2.

2.6 | Immunohistochemistry

2.6.1 | Ionized calcium-binding adapter molecule 1

Iba1 was used to visualize and quantify microglia in brain sections (Imai et al., 1996; Ito et al., 1998). All immunohistochemistry procedures utilized 0.01 M PBS as a diluent and for rinsing. Following PBS rinses (3 × 10 min), sections were placed in methanol containing 0.3% H_2O_2 for 30 min. Sections were rinsed (3 × 10 min); blocked for 1 h in 2% normal goat serum (NGS), 1% bovine serum albumin, and 0.3% triton; and then incubated for 36 h with a rabbit anti-Iba1 polyclonal antibody (1:10,000, Wako, Cat. # 019-19741, RRID: AB_839504) at 4°C.

2.6.2 | Glial fibrillary acidic protein

GFAP with an accompanying Nissl stain was used for astrocyte quantification (Riquier & Sollars, 2020). Following PBS rinses (5 × 5 min 0.2% Triton X-100), sections were blocked in 5% NGS for 90 min, incubated with rabbit anti-GFAP antibody (1:13,000, Abcam, Cat. # ab7260, RRID: AB_305808), and then rinsed and blocked for 30 min in methanol containing 0.3% H_2O_2.

Following three rinses, both Iba1 and GFAP sections were placed in a goat anti-rabbit antibody solution containing 2% NGS and 0.3% Triton X-100 for 2 h at room temperature (1:1000, Vector Laboratories, Cat. # BA-1000, RRID: AB_2313606). Sections were rinsed and then visualized using a 2% avidin–biotin complex solution containing 0.1% Triton X-100 (Vector Laboratories, Burlingame, CA) for 1 h followed by a 0.05% diaminobenzidine solution containing 0.125% nickel ammonium sulfate and 0.01% H_2O_2. Every immunohistochemistry run contained negative control sections that were processed identically to experimental tissue except for omission of the primary or secondary antibody. No staining was observed on negative control tissue.

2.7 | Microscopy

Terminal field tracings and microglia quantification were performed in the NTS of the medulla, the first central relay location for gustatory GL fibers. All visualization, brain region identification, cell counts, and terminal field tracings were performed using a brightfield microscope with the software Neurolucida (RRID:SCR_001775) and NeuroExplorer (RRID:SCR_001818; MBF Bioscience, Williston, VT; https://www.mbfbioscience.com).

2.7.1 | NTS identification and dorsal–ventral zone categorization

The NTS and solitary tract were visualized using phase contrast (Martin et al., 2019; Riquier & Sollars, 2020). The intermediate zone was classified as one section before and after solitary tract passes through the rostral-most portion of the NTS, for a total of three sections (150 μm; Riquier & Sollars, 2017, 2020). All sections dorsal and ventral from the intermediate zone were classified as the dorsal and ventral zones, respectively. Label was typically observed in three to five dorsal zone sections and two to three ventral zone sections.

2.7.2 | Cell counts and correction

Cell counts were performed in the NTS using a 20× (1.6) objective and by placing Neurolucida overlay markers on all Iba1+ cell bodies (microglia) or the Nissl-stained nucleolus of GFAP+ cells (astrocytes). Cells were only counted if the cell body was entirely in the NTS, and all counting was conducted by trained researchers blind to experimental conditions. Due to variability in microglia sizes, Abercrombie corrections (Abercrombie, 1946) to minimize potential overcounting were conducted using the formula: Corrected Counts = Raw Counts × (section thickness/[section thickness + cell height]). Heights of microglia were determined by carefully measuring soma diameters of ~5% of randomly selected cells from control animals of each age. A single mean height for each cell type was calculated for each age for use in the correction. Astrocyte and corrected microglia quantities were converted to densities for analyses by dividing them by the volume of the NTS, calculated by multiplying the counting area of the NTS by the section thickness of 40 μm.

2.7.3 | Terminal field tracing

Terminal field volumes were determined by tracing the outline of BDA-labeled fibers in Neurolucida using a 10× (1.6) objective. Care was taken to only include fibers that clearly expressed terminal boutons and to exclude incoming nerve axons. The midline caudal from the fourth ventricle was used as the limit for fiber tracings. Once terminal field areas were quantified, these values were multiplied by 50 (the section thickness in m) to calculate the terminal field volume.

2.7.4 | Control for nonspecific labeling

To control for the possibility that any increased or abnormal labeling observed may be due to the absorption and

transport of the BDA by nerves near the GL labeling site, a PLX5622-treated P25 animal underwent the labeling procedure described above, but the GL was not cut, and BDA was liberally applied to the area. After allowing 48 h to transport, no BDA was observed in the NTS, suggesting all BDA labels observed in experimental animals were the result of GL fibers.

2.7.5 | Control for increased transport distance

As was expected (reviewed in Hume et al., 2020), by P27 vehicle rats were significantly larger (67.513 ± 1.999 g; $n = 6$) than PLX5622 rats (55.882 ± 2.129 g; $n = 6$; $t_{(10)} = 4.324$, $p = .002$, $d = 2.30$). By P42, PLX5622 rats weighed less than half that of controls (PLX: 85.116 ± 8.125 g; $n = 8$; vehicle: 183.337 ± 8.977 g; $n = 6$; $t_{(12)} = 8.057$, $p < .001$, $d = 4.35$). Thus, it was possible that any differences seen in label quantity may have been due to varying sizes (and thus transport distances). To see if allowing a longer transport time accounted for any differences, two untreated P53 rats were labeled but the label was allowed 72 h to transport before processing. The GL NTS terminal field volumes of these rats ($3.9^{E7} \pm 7^{E6}$; $n = 2$) did not differ from those of approximately age-matched vehicle-treated rats with 48-h transport time ($5.3^{E7} \pm 1^{E7}$; $n = 5$; $t_{(5)} = 0.831$, $p = .444$, $d = 0.70$) indicating that allowing longer for label transport did not result in increased label presence.

2.8 | Data analysis

All analyses were performed using SPSS 25 (RRID:SCR_002865, IBM, Armonk, NY) and graphs were prepared in GraphPad Prism (RRID: SCR_002798). The unit of analysis was always one animal, with the sample size for each analysis expressed as n. Sample sizes were estimated based on our previous studies in rats examining NTS microglia (Riquier & Sollars, 2017, 2020) and NTS terminal fields (Martin et al., 2019). All data were treated as independent/between-subjects factors for analyses, and no collected data were omitted. Between-subjects ANOVAs were performed with independent samples t-tests used for planned comparisons and post hoc tests. All analyses were conducted twice using both parametric and nonparametric tests. These were not different in their outcome, so we are reporting only the parametric results. Results are presented as mean $\pm$ standard error of the mean (SEM), and an alpha level of .05 was used. Sexes were combined for analyses, as no differences between males and females for any measure were detected (ps $> .1$). Terminal field data are expressed in cubic microns (μm^3) and are referred to by the label age, while microglia and astrocyte quantities represent perfusion age.

Microglia and astrocyte densities are expressed as cells per 200,000 μm^3.

3 | RESULTS

3.1 | The gustatory GL terminal field prunes during development, driven by terminal field reduction in the dorsal zone

Independent samples t-tests revealed that for vehicle animals, total NTS GL terminal field volumes were largest at P14 ($1.5^{E8} \pm 2^{E7}$; $n = 4$), decreased by ~50% by P25 ($7.8^{E7} \pm 1^{E7}$; $n = 4$; $t_{(3)} = 3.033$, $p = .023$, $d = 2.14$), and then remained stable through P40 ($5.2^{E7} \pm 1^{E7}$; $n = 5$; $t_{(7)} = 1.547$, $p = .166$, $d = 1.04$; Figure 1a–f,q). Throughout development, the vast majority of the GL terminal field is present in the dorsal zone of the NTS (Figure 1a,c,e), with comparably little in the intermediate zone (Figure 1b,d,f). Thus, the pruning observed between P14 and P25 was driven entirely by substantial terminal field loss in the dorsal zone (ns $= 4$; $t_{(6)} = 2.757$, $p = .033$, $d = 1.94$; Figure 1r). Pruning was observed in the intermediate zone between P25 and P40 (ns $= 4$ and 5, respectively; $t_{(7)} = 2.570$, $p = .037$, $d = 1.72$; Figure 1s), although the total terminal field volume was not significantly affected, likely due to the relatively small amount of terminal field there.

3.2 | While NTS astrocyte quantity remains stable, microglia density in the NTS is highest during the GL pruning period, then decreases when pruning is complete

Elevated quantities of microglia and astrocytes during development are implicated in developmental pruning (Bialas & Stevens, 2013; reviewed in Bosworth & Allen, 2017; reviewed in Schafer & Stevens, 2015). Due to the observed pruning of the GL terminal field between P14 and P25, we next assessed microglia and astrocyte density in the NTS at P11–12 (microglia), P14 (astrocytes), P17 (microglia), P25 (both), and P31–40 (both). See Table 1 for a full list of conditions and n values. There was no significant main effect of age on NTS astrocyte density (ns $= 9$–10; $F_{(2, 27)} = 1.499$, $p > .1$), indicating that astrocyte density remains consistent in the NTS between P14 and P31–40 (Figure 2). However, there was a significant main effect of age on the density of microglia (ns $= 4$–7; $F_{(3, 16)} = 16.783$, $p < .001$, $\eta_{partial}^2 = .759$), suggesting microglia densities change across development. Post hoc independent samples t-tests revealed microglia densities did not differ between P11–12 (2.069 ± 0.07; $n = 7$) and P17 (1.903 ± 0.084; $n = 4$; $t_{(9)} = 1.474$, $p = .175$, $d = 0.92$). By P25 (1.391 ± 0.113; $n = 4$), microglia densities had decreased
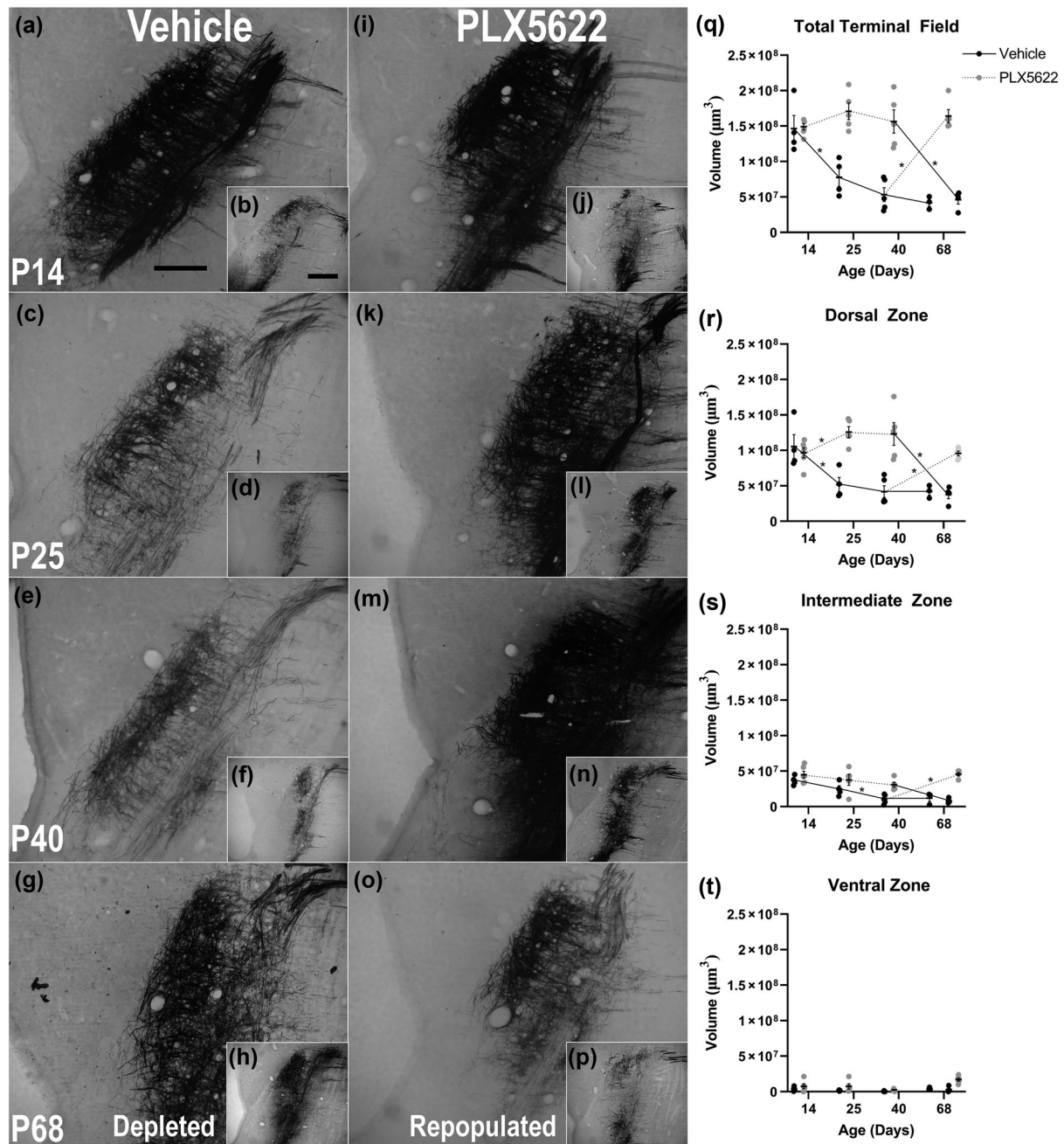
FIGURE 1 Microglia dictate the timing of GL developmental pruning. Images show the GL terminal field across development in both vehicle-treated (a–f) and PLX5622-treated (i–n) rats. The large images display the dorsal zone of the NTS and inserts show the intermediate zone. Panel (q) shows the associated total terminal field volumes (mean ± SEM) and panels (r–t) the distribution by dorsal–ventral zones. Each circle represents a single animal. The bottom row of images shows the terminal field of adult rats that were either treated (g, h) or ceased treatment (u, p) of PLX5622 starting at postnatal day 40 (P40). Asterisk (*) indicates significantly different from the previous timepoint. The large image scale bar is 250 μm, and the insert scale bar is 500 μm.

by approximately 25% ($t_{(6)} = 3.628$, $p = .011$, $d = 2.57$) and continued to remain stable through P31–40 (1.234 ± 0.123; $n = 5$; $t_{(7)} = 0.624$, $p = .552$, $d = 0.42$; Figure 2). These data show that microglia densities in the NTS are highest during GL pruning and decrease after pruning is complete. Taken together, microglia density, but not astrocyte density, corresponds with the timing of developmental pruning of the GL.

3.3 | Microglia are rapidly, profoundly, and chronically depleted in the developing rat brain with daily intraperitoneal injections of PLX5622

Given that we associated microglia quantity with the timing of GL pruning, we next wanted to deplete microglia to determine
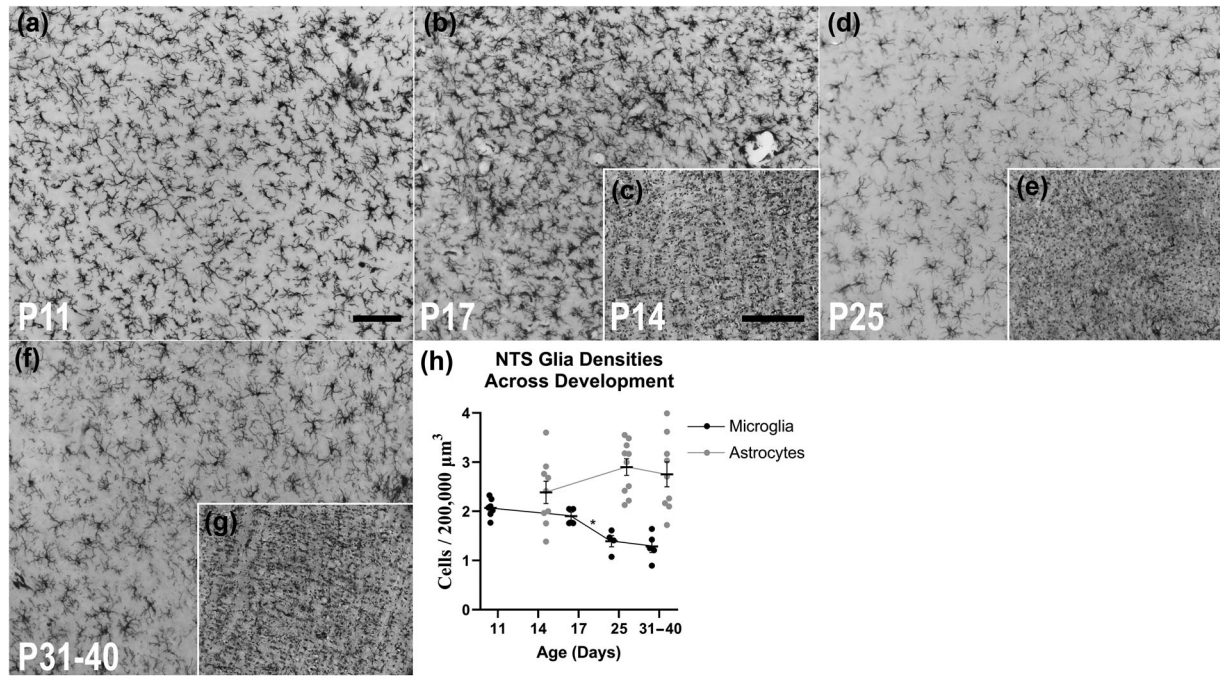
FIGURE 2 Microglia and astrocytes in the rat nucleus of the solitary tract across development. The large images show microglia, and the inserts show astrocytes. At the youngest ages we examined, astrocyte density was approximately 20% greater than that of microglia. While astrocyte density did not change between postnatal day 14 (P14) and P31–P40, microglia density decreased between P17 and P25 (h; Mean ± SEM), leading to a density disparity with approximately 55% greater density of astrocytes as compared to microglia. *p = .011. The microglia scale bar is 100 μm, and the astrocyte scale bar is 250 μm.

their necessity for pruning. Within 3 days of treatment starting at P1, microglia were depleted by >97% in pups treated with PLX5622 (PLX; 0.027 ± 0.012, n = 4; Figure 3a) relative to age-matched vehicle-treated controls (0.89 ± 0.068; n = 2; $t_{(4)}$ = 19.002, p < .001, d = 16.46). Depletion rose to ~99% by P14 (PLX: 0.02 ± 0.004; n = 6; vehicle: 2.098 ± 0.214; n = 5; $t_{(9)}$ = 10.781, p < .001, d = 6.53) and remained stable through P24 (PLX: 0.016 ± 0.004; n = 5; vehicle: 1.489 ± 0.09; n = 0.09; $t_{(8)}$ = 16.409, p < .001, d = 10.38) and P40 (PLX: 0.045 ± 0.013; n = 5; vehicle: 1.526 ± 0.166; n = 5; $t_{(8)}$ = 8.880, p < .001, d = 5.62; Figure 3b,e). Adjacent sections were also labeled for astrocytes, which were not impacted by chronic PLX treatments (Figure 3c), similar to prior work with acute treatments (Riquier & Sollars, 2020). Despite being depleted P4–40, microglia repopulated the brain to control densities within 3 days of ceasing PLX injections (1.4802 ± 0.216; n = 3; $t_{(6)}$ = 0.167, p = .873, d = 0.12; Figure 3d). In addition to the NTS, qualitatively comparable findings were observed in cortical and hippocampal sections, consistent with the systematic depletion present with other methods of CSF1R inhibitor administration (e.g., Elmore et al., 2015; Rice et al., 2015).
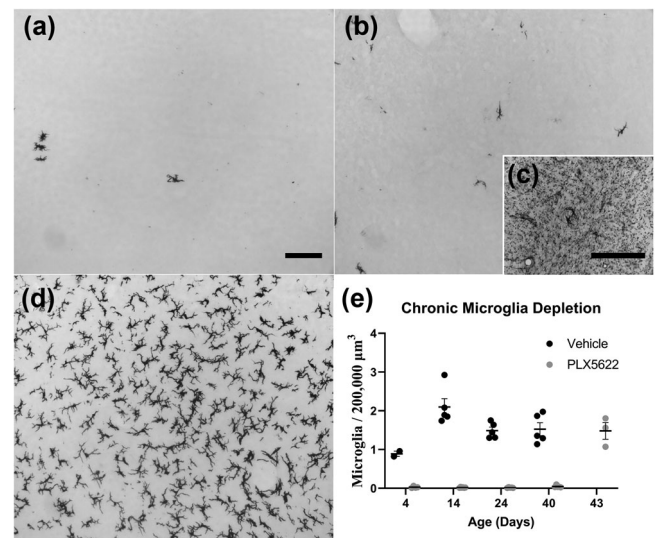
FIGURE 3 Microglia densities following treatment with PLX5622 (gray) or a vehicle injection (black) expressed as mean ± SEM, with each circle representing a single animal. When treatments start at 1 day of age (P1), microglia are rapidly depleted by P4 (a) and remained depleted through P40 (b), while astrocytes are unaffected (c). Once treatments stop at P40, microglia return to control quantities by P43 (d). The microglia scale bar is 100 μm, and the astrocyte scale bar is 250 μm.

3.4 | Microglia depletion with PLX5622 prevents developmental NTS GL pruning and the terminal field expands in the dorsal zone

A between-subjects ANOVA indicated a significant interaction between treatment and age ($n = 29$; $F_{(2, 23)} = 10.106$, $p = .001$, $\eta_{partial}^2 = .468$), suggesting that the effect of age on the pruning of the GL terminal field depended on whether animals were treated with PLX or vehicle. Unlike control rats, animals whose microglia were depleted with PLX had stable total terminal field volumes between P14 ($1.5^{E8} \pm 5^{E6}$; $n = 6$) and P40 ($1.6^{E8} \pm 2^{E7}$; $n = 5$; $t_{(9)} = 0.478$, $p = .644$, $d = 0.29$; Figure 1i–n,q). In contrast to vehicle rats that exhibited pruning primarily in the dorsal NTS zone, the GL terminal field of PLX rats expanded in the dorsal zone between P14 ($9.7^{E7} \pm 7^{E6}$; $n = 6$) and P25 ($1.3^{E8} \pm 8^{E6}$; $n = 5$; $t_{(9)} = 2.747$, $p = .023$, $d = 1.66$) and remained stable through P40 ($1.2^{E8} \pm 2^{E7}$; $n = 5$; $t_{(8)} = 0.144$, $p = .889$, $d = 0.09$; Figure 1r). Taken together, these results suggest that microglia depletion prevented the typical GL terminal field volume reduction that occurs during development.

3.5 | Microglia repopulation allows PLX5622 late-life gustatory GL pruning

Twenty-eight days after ceasing treatments, the terminal field volumes of former vehicle-treated rats ($4.2^{E7} \pm 5^{E6}$; $n = 3$) were similar to those of vehicle animals at P40 ($5.3^{E7} \pm 1^{E7}$; $n = 5$; $t_{(6)} = 0.826$, $p = .440$, $d = 0.60$) and P25 ($7.7^{E7} \pm 1^{E7}$; $n = 4$; $t_{(5)} = 2.244$, $p = .074$, $d = 1.72$; Figure 1q), suggesting that GL pruning had completed by P25. After 28 days of microglia repopulation, the NTS GL terminal field of animals previously treated with PLX had reduced to a volume ($4.6^{E7} \pm 6^{E6}$; $n = 4$) comparable to P40 vehicle animals ($t_{(7)} = 0.561$, $p = .592$, $d = 0.38$) and was no longer different from age-matched controls ($t_{(5)} = 0.490$, $p = .645$, $d = 0.37$; Figure 1o–q). Further, the GL terminal field volume in the dorsal NTS zone of P68 former PLX rats ($3.7^{E7} \pm 5.8^{E6}$; $n = 4$) had reduced to a size similar to controls ($4.1^{E7} \pm 8.3^{E6}$; $n = 5$; $t_{(7)} = 0.402$, $p = .70$, $d = 0.42$; Figure 1r). These results indicate that microglia repopulation outside the normal GL pruning period was sufficient for GL terminal field pruning.

3.6 | Depleting microglia in adulthood reverses previous developmental pruning

Having demonstrated that microglia are required for GL pruning, and that such pruning can occur both developmentally and in adulthood, we next asked if microglia were not just pruning, but continuously maintaining the GL terminal field at a reduced size. To answer this question, we took rats that had already undergone developmental pruning, and treated them with PLX5622 starting at P40. After 4 weeks of treatment, the GL terminal field had expanded to a total volume ($1.7^{E8} \pm 1^{E7}$; $n = 5$; Figure 1g,h,q) comparable to that of prepruning P14 vehicle rats ($1.5^{E8} \pm 2^{E7}$; $n = 4$; $t_{(7)} = 0.961$, $p = .625$, $d = 0.61$) and P40 PLX rats whose pruning had been prevented ($1.6^{E+8} \pm 2^{E7}$; $n = 5$; $t_{(8)} = 0.529$, $p = .460$, $d = 0.30$). These expanded terminal fields were significantly larger overall than postpruning vehicle controls at P25 ($7.8^{E7} \pm 1^{E7}$; $n = 4$; $t_{(7)} = 4.840$, $p = .002$, $d = 3.31$), P40 ($5.2^{E7} \pm 1^{E7}$; $n = 5$; $t_{(8)} = 7.035$, $p = .0001$, $d = 4.46$), and P68 ($4.2^{E7} \pm 5^{E6}$; $n = 3$; $t_{(6)} = 7.086$, $p = .0003$, $d = 5.28$), as well as rats whose terminal field had pruned later in life following microglia repletion ($4.6^{E7} \pm 6^{E6}$; $n = 4$; $t_{(7)} = 7.706$, $p = .0001$, $d = 5.27$). While this expansion occurred in all NTS zones ($ps < .01$), the majority of expansion occured in the dorsal zone, where most of the GL fibers are located (Figure 1r). Depleting microglia in adulthood therefore resulted in terminal fields reverting to their prepruned, expanded state.

3.7 | Microglia maintenance of the GL is limited to NTS-projecting fibers

In addition to projecting gustatory fibers to the NTS, the GL also contains somatosensory fibers that project to the spinal trigeminal nucleus (SPV). To determine if the GL terminal field maintenance function of microglia applied to both fiber types and nuclei, we repeated the developmental microglia depletion and subsequent repopulation analyses on labeled GL fibers in the SPV. As expected, the GL terminal field in the SPV reduced in volume in vehicle animals between P14 ($5.3^{E7} \pm 9^{E6}$; $n = 3$) and P40 ($2.5^{E7} \pm 2^{E6}$; $n = 4$; $t_{(5)} = 3.433$, $p = .019$, $d = 1.68$), and pruning was prevented in PLX rats (P14: $6^{E7} \pm 4^{E6}$; $n = 5$; P40: $5.8^{E7} \pm 6^{E6}$; $n = 4$; $t_{(7)} = 0.227$, $p = .827$, $d = 0.15$; Figure 4). Unlike in the NTS, however, 4 weeks after microglia repopulation the GL terminal field in the SPV of former PLX rats ($4.5^{E7} \pm 2^{E5}$, $n = 3$) had not reduced in size since P40 ($t_{(5)} = 1.992$, $p = .103$, $d = 1.52$), suggesting that preventing GL pruning during development is potentially permanent for somatosensory fibers in the SPV.

4 | DISCUSSION

Here, we report novel data regarding the contribution of microglia and astrocytes to the development and maintenance of the rat GL terminal field. We observed that astrocyte quantity is stable from P11 to P40, and their presence alone is insufficient for pruning of the GL. The present report is the first demonstration that microglia are required for developmental pruning of rat NTS GL fibers, and that such pruning
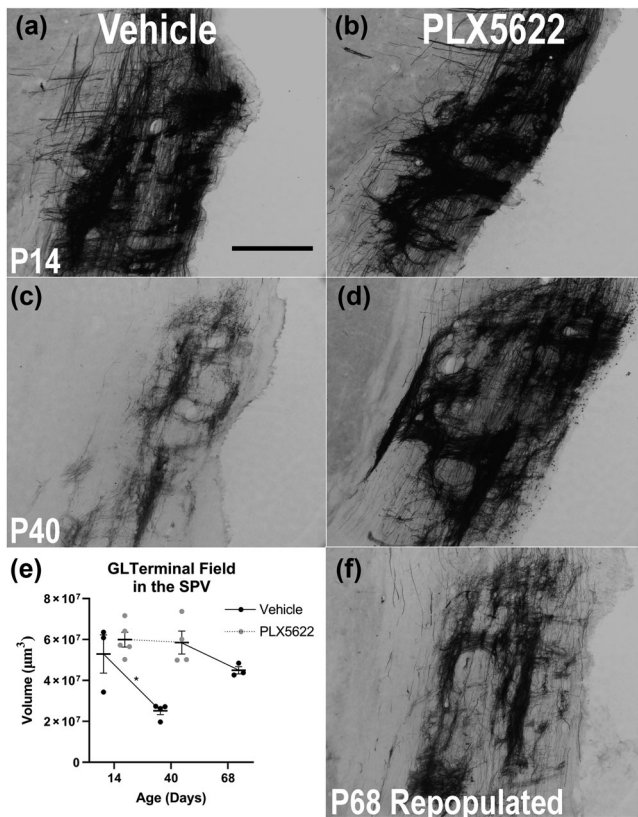
FIGURE 4 Microglia prune the somatosensory fibers of the GL that project to the SPV. This pruning occurs between postnatal day 14 (P14) and P40 (a, c, e; mean ± SEM). Removing microglia with PLX5622 prevents this pruning (b, d, e), which is permanent even with microglia replenishment (e, f). *p = .019. The scale bar is 500 μm.

can occur weeks outside the typical pruning period of P15–25. Additionally, we have also shown that when microglia are depleted from the adult rat brain, this pruning process is reversed, resulting in terminal fields that expand to prepruning sizes. Cumulatively, our findings suggest that the canonical pruning period of the GL is fluid and may in fact just indicate the onset of a lifelong process of microglia maintaining the GL terminal field at a fraction of its maximum size.

4.1 | Microglia are required for developmental GL gustatory terminal field pruning

Consistent with previous reports (Mangold & Hill, 2008), the present data indicate the GL terminal field reduces in volume by approximately 50% between P15 and P25, a period corresponding with a decrease in the elevated NTS microglia density present at P15 (Riquier & Sollars, 2017). Elevated microglia in a noninjured, developing brain are often associated with pruning (Nikodemova et al., 2015; reviewed in Schafer & Stevens, 2015; Sun et al., 2019). Here, we demon-

strate that depletion of microglia with PLX5622 from P1 to P40 prevented GL terminal field pruning from occurring. Further, PLX5622-treated rats had larger GL terminal fields in the dorsal zone of the NTS, the zone where nearly all developmental pruning was observed in controls. A lack of GL pruning in rats is also inducible via embryonic sodium depletion (Mangold & Hill, 2008), which has been shown in mice to permanently reduce NTS microglia quantities and inhibit pruning of the gustatory chorda tympani and greater superficial petrosal nerves (Sun et al., 2019). We report here that NTS microglia density remains elevated until at least P17, further narrowing the window of their developmental decrease. While both microglia and the GL terminal field reach their "mature" states by P25, it is possible that the GL terminal field prunes early within the P15–P25 window after which microglia density decreases.

Microglia prune via the classical complement pathway in an activity-dependent manner (Paolicelli et al., 2011; Schafer et al., 2012; Stevens et al., 2007; Sun et al., 2019). In mice, pruning of the gustatory branches of the facial nerve is microglia and complement dependent (Sun et al., 2019). We are the first to demonstrate that developmental GL pruning in the rat is also microglia dependent. This pruning coincides with an increase in taste input to the NTS (Hill et al., 1983), a developmental increase in GL-innervated taste buds (Hosley & Oakley, 1987), and maturation of taste preferences (Inui-Yamamoto et al., 2017; Midkiff & Bernstein, 1983; Sollars & Bernstein, 1994), suggesting that GL pruning in the rat is likely activity and complement dependent as well.

Altering taste system development can change taste system function, which may be reflected in preference behaviors and in neurophysiological response profiles of NTS cells or higher order neurons. Disrupting taste input by removing the rat chorda tympani during early life (≤P10) has lifelong consequences, resulting in a permanent change in GL function (Martin & Sollars, 2015), alterations in the neurophysiological responses of parabrachial nucleus neurons (Martin et al., 2021) and taste-preference changes (Sollars & Bernstein, 1996). By preventing the pruning of the GL terminal field, it is plausible that the coding of taste information is altered, perhaps influencing the maturation of taste preferences.

4.2 | Microglia dictate GL terminal field malleability in adulthood

While depleting microglia from P1 to P40 prevented developmental GL pruning, 4 weeks after microglia repopulation GL NTS terminal fields had pruned to control volumes, primarily in the dorsal zone. The similarity in NTS terminal field volume between P25 vehicle and P68 former vehicle rats indicates that GL pruning typically stops at P25, yet our data show that microglia will resume pruning at P40 if previously

prevented from doing so. In addition to this "delayed pruning," depleting microglia in adult rats resulted in an expansion of the GL terminal field to prepruning sizes, reversing the pruning process. These results cumulatively demonstrate that microglia are capable of pruning outside of the canonical GL pruning period of P15–P25 and, after pruning is complete, may actively maintain the GL at a reduced size. Confirmation of this interpretation could be explored by attempting repeated pruning cycles, where microglia are once again depleted after delayed pruning. The malleability of gustatory GL fibers did not extend to somatosensory fibers, as repopulated microglia did not resume pruning in the SPV. The lifelong plasticity of the gustatory GL fibers is likely adaptive, as taste receptor cells turn over on average every 11–14 days (Beidler & Smallman, 1965; Perea-Martinez et al., 2013), necessitating fibers to dynamically re-establish synapses throughout the life span. Though outside the scope of our current study, it would be interesting to determine if taste coding is altered with the absence of microglia and if expansive outgrowth of gustatory fibers in adult rats that already experienced normal developmental pruning results in a functionally and behaviorally immature system.

Our results suggest that instead of developmental pruning leading to a stable, mature terminal field size that fluctuates moderately in response to taste receptor cell turnover, it appears the default of these sensory fibers is a drive toward expansion, with microglia continually keeping them at a stable state. In our current study, we found that a ∼99% absence of microglia in the NTS leads to release of constraint on the expansive growth of gustatory fibers. Permissive expansion of gustatory terminal fields has been observed following various other manipulations (Corson & Hill, 2011; Skyberg et al., 2017; Sun et al., 2018), all of which likely directly or indirectly impact microglia (Eriksson et al., 1993; Hung et al., 2010; Zhang et al., 2014). While the taste system is particularly dynamic, the need to balance stability along with flexibility to adapt across the life span is required for many systems (reviewed in Yin & Yuan, 2015). Lifelong plasticity necessitates a constantly evolving interplay between permissive neural outgrowth and constrictive factors to maintain constancy in the midst of a fluidic system. While many factors likely contribute to this capability, our results add to evidence that microglia are likely a substantial, if not primary, contributor.

5 | CONCLUSIONS

Here, we provide data on the effects of chronic CSF1R inhibition on pruning and maintenance of the rat GL terminal field. We show that depleting microglia with PLX5622 either during development or in adulthood results in either a prevention or reversal of GL pruning, respectively. When pruning is

prevented, allowing microglia to return in adulthood resumes pruning, restoring the GL terminal field to a size equivalent to normally developed rats. These data, in conjunction with previous work (Mangold & Hill, 2008; May & Hill, 2006; Sun et al., 2019), suggest microglia not only prune, but may continuously suppress the size of the GL terminal field. These data provide novel insight regarding microglia in the developing brain as well as their role in central fiber maintenance and lifelong neuroplasticity.

CONFLICT OF INTEREST
The authors declare no conflict of interest.

DATA AVAILABILITY STATEMENT
The data that support the findings of this study are available from the corresponding author upon reasonable request.

ORCID
Andrew J. Riquier https://orcid.org/0000-0001-9470-5949

REFERENCES
Abercrombie, M. (1946). Estimation of nuclear population from microtome sections. *The Anatomical Record*, *94*, 239–247. https://doi.org/10.1002/ar.1090940210

Askew, K., Li, K., Olmos-Alonso, A., Garcia-Moreno, F., Liang, Y., Richardson, P., Tipton, T., Chapman, M. A., Riecken, K., Beccari, S., Sierra, A., Molnár, Z., Cragg, M. S., Garaschuk, O., Perry, V. H., & Gomez-Nicola, D. (2017). Coupled proliferation and apoptosis maintain the rapid turnover of microglia in the adult brain. *Cell Reports*, *18*, 391–405. https://doi.org/10.1016/j.celrep.2016.12.041

Beidler, L. M., & Smallman, R. L. (1965). Renewal of cells within taste buds. *Journal of Cell Biology*, *27*(2), 263–272. https://doi.org/10.1083/jcb.27.2.263

Bialas, A. R., & Stevens, B. (2013). TGF-*β* signaling regulates neuronal C1q expression and developmental synaptic refinement.

Nature Neuroscience, *16*, 1773–1782. https://doi.org/10.1038/nn.3560

Bosworth, A. P., & Allen, N. J. (2017). The diverse actions of astrocytes during synaptic development. *Current Opinion in Neurobiology*, *46*, 38–43. https://doi.org/10.1016/j.conb.2017.08.017

Bruttger, J., Karram, K., Wörtge, S., Regen, T., Marini, F., Hoppmann, N., Klein, M., Blank, T., Yona, S., Wolf, Y., Mack, M., Pinteaux, E., Müller, W., Zipp, F., Binder, H., Bopp, T., Prinz, M., Jung, S., & Waisman, A. (2015). Genetic cell ablation reveals clusters of local self-renewing microglia in the mammalian central nervous system. *Immunity*, *43*, 92–106. https://doi.org/10.1016/j.immuni.2015.06.012

Chung, W., Clarke, L. E., Wang, G. X., Stafford, B. K., Sher, A., Chakraborty, C., Joung, J., Foo, L. C., Thomspon, A., Chen, C., Smith, S. J., & Barres, B. A. (2013). Astrocytes mediate synapse elimination through MEGF10 and MERTK pathways. *Nature*, *504*(7480), 394–400. https://doi.org/10.1038/nature12776

Corson, S. L., & Hill, D. L. (2011). Chorda tympani nerve terminal field maturation and maintenance is severely altered following changes to gustatory nerve input to the nucleus of the solitary tract. *Journal of Neuroscience*, *31*(21), 7591–7603. https://doi.org/10.1523/JNEUROSCI.0151-11.2011

Elmore, M. R., Lee, R. J., West, B. L., & Green, K. N. (2015). Characterizing newly repopulated microglia in the adult mouse: Impacts on animal behavior, cell morphology, and neuroinflammation. *PLoS One*, *10*(4), e0122912. https://doi.org/10.1371/journal.pone.0122912

Eriksson, N. P., Persson, J. K., Svensson, M., Arvidsson, J., Molander, C., & Aldskogius, H. (1993). A quantitative analysis of the microglial cell reaction in central primary sensory projection territories following peripheral nerve injury in the adult rat. *Experimental Brain Research*, *96*(1), 19–27. https://doi.org/10.1007/BF00230435

Hashimoto, K., & Kano, M. (2003). Functional differentiation of multiple climbing fiber inputs during synapse elimination in the developing cerebellum. *Neuron*, *38*(5), 785–796. https://doi.org/10.1016/s0896-6273(03)00298-8

Hashimoto, K., & Kano, M. (2013). Synapse elimination in the developing cerebellum. *Cellular and Molecular Life Sciences*, *70*(24), 4667–4680. https://doi.org/10.1007/s00018-013-1405-2

Hill, D. L., Bradley, R. M., & Mistretta, C. M. (1983). Development of taste responses in rat nucleus of solitary tract. *Journal of Neurophysiology*, *50*(4), 879–895. https://doi.org/10.1152/jn.1983.50.4.879

Hoshiko, M., Arnoux, I., Avignone, E., Yamamoto, N., & Audinat, E. (2012). Deficiency of the microglial receptor CX3CR1 impairs postnatal functional development of thalamocortical synapses in the barrel cortex. *Journal of Neuroscience*, *32*, 15106–15111. https://doi.org/10.1523/JNEUROSCI.1167-12.2012

Hosley, M. A., & Oakley, B. (1987). Postnatal development of the vallate papilla and taste buds in rats. *The Anatomical Record*, *218*(2), 216–222. https://doi.org/10.1002/ar.1092180217

Huberman, A. D. (2007). Mechanisms of eye-specific visual circuit development. *Current Opinion in Neurobiology*, *17*(1), 73–80. https://doi.org/10.1016/j.conb.2007.01.005

Hume, D. A., Caruso, M., Ferrari-Cestari, M., Summers, K. M., Pridans, C., & Irvine, K. M. (2020). Phenotypic impacts of CSF1R deficiencies in humans and model organisms. *Journal of Leukocyte Biology*, *107*(2), 205–219. https://doi.org/10.1002/JLB.MR0519-143R

Hung, J., Chansard, M., Ousman, S. S., Nguyen, M. D., & Colicos, M. A. (2010). Activation of microglia by neuronal activity: Results from a new in vitro paradigm based on neuronal-silicon interfacing technology. *Brain, Behavior, and Immunity*, *23*(1), 31–40. https://doi.org/10.1016/j.bbi.2009.06.150

Imai, Y., Ibata, I., Ito, D., Ohsawa, K., & Kohsaka, S. (1996). A novel gene iba1 in the major histocompatibility complex class III region encoding an EF hand protein expressed in a monocytic lineage. *Biochemical and Biophysical Research Communications*, *224*(3), 855–862. https://doi.org/10.1006/bbrc.1996.1112

Innocenti, G. M. (1981). Growth and reshaping of axons in the establishment of visual callosal connections. *Science*, *212*(4496), 824–827. https://doi.org/10.1126/science.7221566

Inui-Yamamoto, C., Yamamoto, T., Ueda, K., Nakatsuka, M., Kumabe, S., Inui, T., & Iwai, Y. (2017). Taste preference changes throughout different life stages in male rats. *PLoS ONE*, *12*(7), e0181650. https://doi.org/10.1371/journal.pone.0181650

Ito, D., Imai, Y., Ohsawa, K., Nakajima, K., Fukuuchi, Y., & Kohsaka, S. (1998). Microglia specific localisation of a novel calcium binding protein, Iba1. *Molecular Brain Research*, *57*(1), 1–9. https://doi.org/10.1016/s0169-328x(98)00040-0

Kierdorf, K., & Prinz, M. (2017). Microglia in steady state. *The Journal of Clinical Investigation*, *127*(9), 3201–3209. https://doi.org/10.1172/JCI90602

Low, L. K., Liu, X. B., Faulkner, R. L., Coble, J., & Cheng, H. J. (2008). Plexin signaling selectively regulates the stereotyped pruning of corticospinal axons from visual cortex. *Proceedings of the National Academy of Sciences of the United States of America*, *105*(23), 8136–8141. https://doi.org/10.1073/pnas.0803849105

Mallya, A. P., Wang, H. D., Lee, H. N. R., & Deutch, A. Y. (2019). Microglial pruning of synapses in the prefrontal cortex during adolescence. *Cerebral Cortex*, *29*(4), 1634–1643. https://doi.org/10.1093/cercor/bhy061

Mangold, J. E., & Hill, D. L. (2008). Postnatal reorganization of primary afferent terminal fields in the rat gustatory brainstem is determined by prenatal dietary history. *Journal of Comparative Neurology*, *509*(6), 594–607. https://doi.org/10.1002/cne.21760

Martin, L. J., Breza, J. M., & Sollars, S. I. (2021). Taste activity in the parabrachial region in adult rats following neonatal chorda tympani transection. *Journal of Neurophysiology*, *125*(6), 2178–2190. https://doi.org/10.1152/jn.00552.2020

Martin, L. J., Lane, A. H., Samson, K. K., & Sollars, S. I. (2019). Regenerative failure following rat neonatal chorda tympani transection is associated with geniculate ganglion cell loss and terminal field plasticity in the nucleus of the solitary tract. *Neuroscience*, *402*, 66–77. https://doi.org/10.1016/j.neuroscience.2019.01.011

Martin, L. J., & Sollars, S. I. (2015). Long-term alterations in peripheral taste responses to NaCl in adult rats following neonatal chorda tympani transection. *Chemical Senses*, *40*(2), 97–108. https://doi.org/10.1093/chemse/bju063

May, O. L., & Hill, D. L. (2006). Gustatory terminal field organization and developmental plasticity in the nucleus of the solitary tract revealed through triple fluorescent labeling. *The Journal of Comparative Neurology*, *497*(4), 658–669. https://doi.org/10.1002/cne.21023

Midkiff, E. E., & Bernstein, I. L. (1983). The influence of age and experience on salt preference of the rat. *Developmental Psychobiology*, *16*(5), 385–394. https://doi.org/10.1002/dev.420160504

Milinkeviciute, G., Henningfield, C. M., Muniak, M. A., Chokr, S. M., Green, K. N., & Cramer, K. A. (2019). Microglia regulate pruning of specialized synapses in the auditory brainstem. *Frontiers in Neural Circuits*, *13*, 55. https://doi.org/10.3389/fncir.2019.00055

Neniskyte, U., & Gross, C. T. (2017). Errant gardeners: Glial-cell-dependent synaptic pruning and neurodevelopmental disorders. *Nature Reviews Neuroscience*, *18*(11), 658–670. https://doi.org/10.1038/nrn.2017.110

Nikodemova, M., Kimyon, R. S., De, I., Small, A. L., Collier, L. S., & Watters, J. J. (2015). Microglial numbers attain adult levels after undergoing a rapid decrease in cell number in the third postnatal week. *Journal of Neuroimmunology*, *278*, 280–288. https://doi.org/10.1016/j.jneuroim.2014.11.018

Paolicelli, R. C., Bolasco, G., Pagani, F., Maggi, L., Scianni, M., Panzanelli, P., Giustetto, M., Ferreira, T. A., Guiducci, E., Dumas, L., Ragozzino, D., & Gross, C. T. (2011). Synaptic pruning by microglia is necessary for normal brain development. *Science*, *333*(6048), 1456–1458. https://doi.org/10.1126/science.1202529

Parkhurst, C. N., Yang, G., Ninan, I., Savas, J. N., Yates, J. R., Lafaille, J. J., Hempstead, B. L., Littman, D. R., & Gan, W. B. (2013). Microglia promote learning-dependent synapse formation through brain-derived neurotrophic factor. *Cell*, *155*(7), 1596–609. https://doi.org/10.1016/j.cell.2013.11.030

Perea-Martinez, I., Nagai, T., & Chaudhari, N. (2013). Functional cell types in taste buds have distinct longevities. *PLoS ONE*, *8*(1), e53399. https://doi.org/10.1371/journal.pone.0053399

Rice, R. A., Spangenberg, E. E., Yamate-Morgan, H., Lee, R. J., Arora, R. P., Hernandez, M. X., Tenner, A. J., West, B. L., & Green, K. N. (2015). Elimination of microglia improves functional outcomes following extensive neuronal loss in the hippocampus. *Journal of Neuroscience*, *35*(27), 9977–9989. https://doi.org/10.1523/JNEUROSCI.0336-15.2015

Riquier, A. J., & Sollars, S. I. (2017). Microglia density decreases in the rat rostral nucleus of the solitary tract across development and increases in an age-dependent manner following denervation. *Neuroscience*, *355*, 36–48. https://doi.org/10.1016/j.neuroscience.2017.04.037

Riquier, A. J., & Sollars, S. I. (2020). Astrocytic response to neural injury is larger during development than in adulthood and is not predicated upon the presence of microglia. *Brain Behavior Immunity-Health*, *1*, 100010. https://doi.org/10.1016/j.bbih.2019.100010

Rosin, J. M., Vora, S. R., & Kurraschabc, D. M. (2018). Depletion of embryonic microglia using the CSF1R inhibitor PLX5622 has adverse sex-specific effects on mice, including accelerated weight gain, hyperactivity and anxiolytic-like behavior. *Brain, Behavior, and Immunity*, *73*, 682–697. https://doi.org/10.1016/j.bbi.2018.07.023

Schafer, D. P., Lehrman, E. K., Kautzman, A. G., Koyama, R., Mardinly, A. R., Yamasaki, R., Ransohoff, R. M., Greenberg, M. E., Barres, B. A., & Stevens, B. (2012). Microglia sculpt postnatal neural circuits in an activity and complement-dependent manner. *Neuron*, *74*(4), 691–705. https://doi.org/10.1016/j.neuron.2012.03.026

Schafer, D. P., & Stevens, B. (2015). Microglia function in central nervous system development and plasticity. *Cold Spring Harbor Perspectives in Biology*, *7*(10), a020545. https://doi.org/10.1101/cshperspect.a020545

Skyberg, R., Sun, C., & Hill, D. L. (2017). Maintenance of mouse gustatory terminal field organization is disrupted following selective removal of peripheral sodium salt taste activity at adulthood. *Journal of Neuroscience*, *37*(32), 7619–7630. https://doi.org/10.1523/JNEUROSCI.3838-16.2017

Sollars, S. I., & Bernstein, I. L. (1994). Amiloride sensitivity in the neonatal rat. *Behavioral Neuroscience*, *108*(5), 981–987. https://doi.org/10.1037//0735-7044.108.5.981

Sollars, S. I., & Bernstein, I. L. (1996). Neonatal chorda tympani transection alters adult preference for ammonium chloride in the rat. *Behavioral Neuroscience*, *110*(3), 551–558.

Sollars, S. I., Walker, B. R., Thaw, A. K., & Hill, D. L. (2006). Age-related decrease of the chorda tympani nerve terminal field in the nucleus of the solitary tract is prevented by dietary sodium restriction during development. *Neuroscience*, *137*(4), 1229–1236. https://doi.org/10.1016/j.neuroscience.2005.09.040

Stevens, B., Allen, N. J., Vazquez, L. E., Howell, G. R., Christopherson, K. S., Nouri, N., Micheva, K. D., Mehalow, A. K., Huberman, A. D., Stafford, B., Sher, A., Litke, A. M., Lambris, J. D., Smith, S. J., John, S. W. M., & Barres, B. A. (2007). The classical complement cascade mediates CNS synapse elimination. *Cell*, *131*(6), 1164–1178. https://doi.org/10.1016/j.cell.2007.10.036

Sun, C., Krimm, R., & Hill, D. L. (2018). Maintenance of mouse gustatory terminal field organization is dependent on BDNF at adulthood. *The Journal of Neuroscience*, *38*(31), 6873–6887. https://doi.org/10.1523/JNEUROSCI.0802-18.2018

Sun, C., Zheng, S., Perry, J. S. A., Norris, G. T., Cheng, M., Kong, F., Skyberg, R., Cang, J. C., Erisir, A., Kipnis, J., & Hill, D. L. (2019). Early gestational maternal diet programs wiring of developing central gustatory circuits by microglia. *SSRN Electronic Journal*, https://doi.org/10.2139/ssrn.3508869

Wang, X., Zhao, L., Zhang, J., Fariss, R. N., Ma, W., Kretschmer, F., Wang, M., Qian, H. H., Badea, T. C., Diamond, J. S., Gan, W. B., Roger, J. E., & Wong, W. T. (2016). Requirement for microglia for the maintenance of synaptic function and integrity in the mature retina. *The Journal of Neuroscience*, *36*(9), 2827–2842. https://doi.org/10.1523/JNEUROSCI.3575-15.2016

Yin, J., & Yuan, Q. (2015). Structural homeostasis in the nervous system: A balancing act for wiring plasticity and stability. *Frontiers in Cellular Neuroscience*, *8*, 439. https://doi.org/10.3389/fncel.2014.00439

Zhang, X., Zeng, L., Yu, T., Xu, Y., Pu, S., Du, D., & Jiang, W. (2014). Positive feedback loop of autocrine BDNF from microglia causes prolonged microglia activation. *Cellular Physiology and Biochemistry*, *34*(3), 715–723. https://doi.org/10.1159/000363036